Talanta 116 (2013) 514–519

Contents lists available at ScienceDirect

Talanta

journal homepage: www.elsevier.com/locate/talanta

Integrated miniature fluorescent probe to leverage the sensing potential of ZnO quantum dots for the detection of copper (II) ions

Sing Muk Ng*, Derrick Sing Nguong Wong, Jane Hui Chiun Phung, Hong Siang Chua

Faculty of Engineering, Computing, and Science, Swinburne University of Technology Sarawak Campus, Jalan Simpang Tiga, 93350 Kuching, Sarawak, Malaysia

ARTICLE INFO

Article history:
Received 3 April 2013
Received in revised form
15 July 2013
Accepted 15 July 2013
Available online 20 July 2013

Keywords:
Miniature fluorescent probe
Quantum-dots
ZnO
Fluorescence
Quenching
Copper (II) ions
Optical sensors

ABSTRACT

Quantum dots are fluorescent semiconductor nanoparticles that can be utilised for sensing applications. This paper evaluates the ability to leverage their analytical potential using an integrated fluorescent sensing probe that is portable, cost effective and simple to handle. ZnO quantum dots were prepared using the simple sol–gel hydrolysis method at ambient conditions and found to be significantly and specifically quenched by copper (II) ions. This ZnO quantum dots system has been incorporated into an in-house developed miniature fluorescent probe for the detection of copper (II) ions in aqueous medium. The probe was developed using a low power handheld black light as excitation source and three photo-detectors as sensor. The sensing chamber placed between the light source and detectors was made of 4-sided clear quartz windows. The chamber was housed within a dark compartment to avoid stray light interference. The probe was operated using a microcontroller (Arduino Uno Revision 3) that has been programmed with the analytical response and the working algorithm of the electronics. The probe was sourced with a 12 V rechargeable battery pack and the analytical readouts were given directly using a LCD display panel. Analytical optimisations of the ZnO quantum dots system and the probe have been performed and further described. The probe was found to have a linear response range up to 0.45 mM (R^2=0.9930) towards copper (II) ion with a limit of detection of 7.68×10^{-7} M. The probe has high repeatable and reliable performance.

1. Introduction

Fluorescence is the basis for large number of bioassays and chemical sensing techniques. The technique usually employs of a fluorophore to interact with an analyte of interest, which later will generate useful and recordable change in its emission signal. This change in signal often correlates to the identity and/or quantity of the analyte of interest. In the early days, fluorophores are extracted directly from natural resources such as plants, while continuous progress has advanced the option into the synthesis of synthetic organic fluorescent dyes in laboratories. The cyanine-based dyes and its derivatives are examples of fluorophores that have been popularly synthesised in-house and used for sensing applications over the past few decades [1,2]. To the most recent development, a new class of fluorophore has been synthesised, better known as the quantum dots (Q-Dots). Q-Dots are colloidal semiconductors in the size range of 1–100 nm, comprised of the elements from the periodic groups II–VI, III–V or IV–VI. Some common examples are zinc oxide, zinc sulphide and cadmium sulphide [3]. Q-Dots exhibit some remarkable properties including high quantum yields and size-tunable emission, chemically and physically more stable, narrow spectral bands, and can be surface modified for an intended application [4]. These unique properties make Q-Dots have more advantages over the conventional organic dyes as fluorophores. Some successful utilisations of Q-Dots are in the areas of urologic oncology [5], labelling [6], bio-imaging [7,8], diagnostic and sensoric [9,10], and medicine [11,12].

Q-Dots can also be adopted as an integrated component within optical assays and sensing systems [13]. Compared to conventional dyes, Q-Dots are relatively more efficient with a quantum yield that is generally over 50% [14]. To date, Q-Dots were reported to detect metal ions [15,16], biological compounds [17], pollutants [18], and even complex species such as DNAs [19]. The majority of these works show low detection limits with considerably good dynamic ranges for the quantification of real samples collected from different areas. In addition, the science behind the sensing interactions has been studied intensively, and several possible sensing mechanisms have been suggested. Some of those mechanisms are electrochemiluminescence, Förster resonance energy transfer, charge transfer, and bioluminescence energy transfer [13,20].

While the analytical potential of Q-Dots is convincing, their practical utilisation for real sensing applications still remain

* Corresponding author. Tel.: +60 82 260848; fax: +60 82 260813.
E-mail address: smng@swinburne.edu.my (S.M. Ng).

0039-9140/$ - see front matter © 2013 Elsevier B.V. All rights reserved.
http://dx.doi.org/10.1016/j.talanta.2013.07.031

a challenge. The major hurdle is on innovating the Q-Dots into a practical working probe that is portable, cheap, robust, reliable, and sufficiently sensitive for in-situ sensing. It is noted that the majority of the Q-Dots sensing systems reported in the literature are developed based on the use of Q-Dots that were integrated onto conventional instrumentation such as spectrofluorometers, fibre optic attachments to spectrophotometers or used of the high performance liquid chromatography. Utilising these well-established instrumentation as sensing transducers no doubt give reliable and consistent results, however they suffer from the drawbacks of expensive running cost and is less portable. The use of a mini-spectrophotometer that is readily available in the market can be an alternative to overcome some of these limitations, but is not significant in terms of the cost. The reason is simply because mini-spectrophotometers are developed for general purposes and thus come with parts of high specifications that are expensive. They usually have CCDs array detectors that cover a full range from UV to visible wavelengths with a wavelength selector and the use of high power UV-light sources. In the context of Q-Dots, high specification parts are not required since the Q-Dots can emit strong fluorescence with considerably wide excitation wavelengths. Thus, a simple in-house setup with basic photo-detector and near UV light source will be sufficient enough to operate the sensing system, which can reduce the cost significantly as compared to the present mini-spectrophotometer.

This work reports the development of an integrated miniature fluorescent sensing probe using Q-Dots as sensing receptor. The aim is to demonstrate a practical application of the Q-Dots for metal ion sensing via simple and cost effective electronic setup without relying on expensive pre-configured optical systems from the market. So far, there are very few studies that focus on this area. The probe was built using low power electronic and operated by rechargeable batteries. Handheld black light was used as the excitation light source instead of deuterium light source that is more expensive and consuming higher power. Meanwhile, light-to-frequency converters were used as photo-detectors to record the change in light intensity of the Q-Dots after being introduced with the analyte. In this system, the Q-Dots showed bright visible emission over a fixed wavelength and thus will not require the use of expensive and wavelength tuneable CCD arrays as detector. The electronic setup of the probe was operated using a simple microcontroller with the final readout being displayed directly on a LCD keypad display. It requires no computer interface to operate the probe. Sensing occurs in a sample compartment made of quartz windows. As a whole, the proposed configuration for the system can reduce the cost significantly while still be able to leverage the analytical potential of the Q-Dots for optical sensing applications.

ZnO Q-Dots have been chosen for this study since it is easier to synthesis and is less toxic compared to the other Q-Dots. Furthermore, the emission of ZnO can be efficiently quenched by cupric ions (Cu (II)), which makes it a potential candidate of analyte for this system. Copper is classified under heavy metal category that has environmental and health concerns and requires efficient sensing systems for its monitoring [21,22]. The fabrication, optimisation and performance of the sensing probe were discussed and described in detail in this work.

2. Experimental

2.1. Reagents and instrumentation

All chemicals used in this study were of analytical grade or higher unless otherwise stated. Double-distilled deionised water and absolute ethanol (Aldrich) were used as solvents throughout the study. Zinc (II) acetate dehydrates, copper (II) nitrate and sodium hydroxide all from Sigma-Aldrich were used as purchased without further purification.

Standard spectrofluormeter (Cary Eclipse, Varian) set under fluorescent mode was used to record the visible emission spectrum of the sample for validation purpose. pH meter (Mettler Toledo SevenEasy) was used to monitor the pH and standard heating mantle with stirrer was used for the reflux purpose. All stirrings were performed using standard PTFE 'Octagon' magnetic bar with the dimension of $25.4 \times 8.0\ mm^2$, with stirring speed at average of 200 rpm.

2.2. ZnO synthesis

ZnO was prepared using room temperature sol–gel chemistry approach in ethanolic media. Absolute ethanol was used to avoid excess amount of water that can terminate the sol–gel process [23]. More information on the influence of solvent on the synthesis can be obtained from the literature [24]. For this study, the ZnO synthesis was performed using the starting precursor of zinc (II) acetate dihydrate that was added in ethanol solvent at a molar-ratio of 1:200 (Zn (II): ethanol) at a total volume of 20 ml. The mixture was then refluxed at 70 °C and it was observed that the solid has dissolved completely in the solvent after 30 min of constant stirring, but formed white precipitate at the end of the 3 h reflux. Wu and co-workers have defined this as first precipitation time [25]. Following this, the mixture was bought to room temperature and further down to approximately 0 °C in ice bath. To this cold mixture, it was added drop-wise with sodium hydroxide solution that has been pre-prepared (0.2 M, 5.0 ml, approximately 0 °C) under constant stirring. The mixture was continuously stirred for another 3 h at low temperature before being repeatedly centrifuged and washed for 3 times using cold ethanol. The finally collected white power was redispersed in ethanol and kept under dark condition for further studies.

2.3. Sensing probes assembly

The sensing probe was designed with a UV light source and 3 light-to-frequency converters (TSL235R-LF) as photo-detectors that were integrated onto a microcontroller as shown in Fig. 1. The compact photo-detector consists of a silicon photodiode and a current-to-frequency converter that are housed in a single monolithic CMOS integrated circuit. The photo-detector responds to light over the range of 320–1050 nm and can be controlled directly

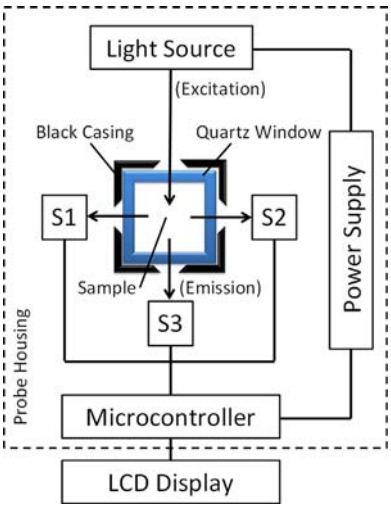

Fig. 1. Schematic diagram showing the different working components of the miniature sensing probe developed in this study.

by the microcontroller using the frequency counter library provided by the manufacture. Photo-detectors S1 and S2 were used to monitor the fluorescence emission intensity, aligned at a fixed '90°-configuration' as referred to the light source. This is to minimise possible interference directly from the light source. The '90°-configuration' has been well adopted in conventional spectro-fluorometers. The third photo-detector, S3 was aligned at a straight path with the light source that serves as a reference sensor. Any spike or deviation caused by the light source can be corrected using this reference sensor. Due to the limited number of digital input/output pins on the microcontroller, a dual 4–1 line selector/multiplexer (CD74HC153E) was used to connect the outputs of the three photo-detectors to the digital pin 5 of the microcontroller. The microcontroller read the output one at a time from the multiplexer. Data processing was performed by the microcontroller based on the analytical calibration relationship in order to evaluate the concentration of Cu (II) ions, which will be displayed on the LCD panel. The connexion of pins allocation of the microcontroller is shown in Fig. 2.

The UV light source was modified from a handheld black light tube (4 W, Philip), which emits UV in the range of 300–420 nm with a maximum intensity of 365 nm. The tube was operated by a single transistor oscillator circuit. In this setup, current will be passed through the primary winding of the yellow inverter transformer, which is a miniature high frequency transformer consisting of a $25 \times 20 \times 5\ mm^3$ ferrite core with 30 turns of primary, 15 turns of feedback and 250 turns of secondary all concentric. This current will induct a magnetic field to the core and the energy will be received back by the feedback windings with a delay. This delay causes the system to oscillate continuously, which subsequently light-up the UV tube.

The prototype probe was powered using Li-ION rechargeable batteries (3.7 V, UltraFire®) that have been connected in series. The supply was regulated using voltage regulators of 6 and 9 V, supplying power to the light source and the microcontroller respectively. Low voltage indicator was also integrated into the system to avoid the unit from running at insufficient power level that can lead to major error on the final signal recorded.

To make it more portable and easier to operate, a direct LCD output display (Arduino-LCD Keypad Shield) was integrated into the probe unit to give a direct readout on the analyte concentration. The display panel consists of a 1602 white character blue backlight 2×16 LCD and operates well with 5 V. The display panel was plugged into the Arduino Uno main board for operation.

2.4. Core control and measurement operational flow

A microcontroller as the core of the probe was used to operate the circuits, coordinate the working flow of the unit, data storage, and data analysis. Arduino Uno Revision 3 microcontroller (obtained from Myduino.com) was chosen as it has well-matched current shields and code with sufficient number of input and output pins (Fig. 2). The microcontroller consists of 14 digital I/O pins and 6 analogue input pins. It was operated using 5 V power supply, which can be powered from a USB connexion or with an external power. Under the external power supply option, an AC-to-DC adaptor can be plugged into the board's power jack or a battery can be connected to the Gnd and Vin pin headers of the power connector. This study used the USB power source during the developmental stage and switched to battery power during the final testing to demonstrate that the probe is portable.

The light intensity detected was converted into a frequency reading and fed into the microcontroller for further analysis. Signal from S3 was used as baseline and all subsequent signals recorded from the S1 and S2 were corrected against it to minimise abnormalities such as noises or spikes in the signal. Besides, S3 was also assigned to monitor the stability of the light source when the unit was switched-on for the first time. Analysis can only be performed once S3 detected a stable intensity emitted from the light source. In terms of data analysis, the standard Stern–Volmer relationship (Eq. (1)) was programmed into the microcontroller to model the response of the sensing system. The operational flow of the probe was given in Fig. 3.

$$F_0/F = Ksv[C] + 1 \quad (1)$$

where F_0 and F are the fluorescence intensities recorded in absence and presence of Cu (II) ions, respectively, [C] is the concentration of Cu (II) ions and Ksv is the Stern–Volmer quenching constant.

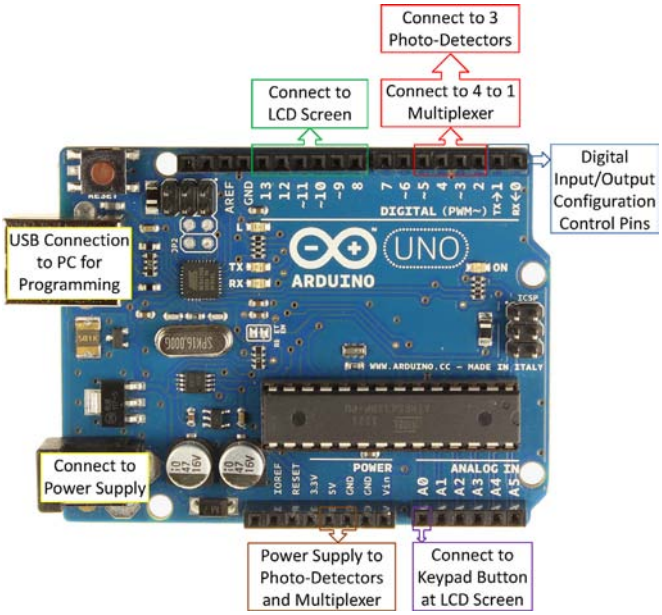

Fig. 2. Microcontroller, Arduino Uno Revision 3 used to operate the sensing probe.

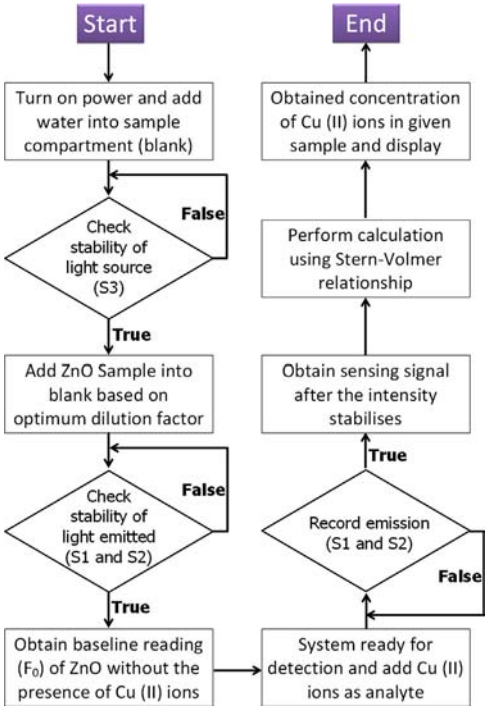

Fig. 3. Operational work flow of the sensing probe.

2.5. Analytical characterisations and optimisations

The initial study on the optical property of the ZnO was carried out using a conventional spectrofluorometer to find out the working optical range of the ZnO that matches the analytical window of the sensing probe. Besides, the analytical potential and quenching mechanism of the ZnO for the sensing of Cu (II) ions were also studied using the same spectrofluorometer. The study focused on establishing the change in signal of the ZnO, especially on the intensity recorded before and once Cu (II) ions was added. In the aspect of setting up the probe, each component and configuration affecting the analytical performance were optimised to obtain the best sensing output for Cu (II) ions.

3. Results and discussion

3.1. ZnO characteristics and quenching profile

A drop of the ZnO in ethanol solution was placed onto an aluminium sheet, dried under vacuum and viewed under a transmission electron microscope (TEM) (JEM 1230). The image (Fig. 4) shows that the distribution of size of the ZnO was very homogenous, in spherical shape and having an average diameter of around 10 nm. The ZnO was also observed to be well dispersed, indicating that the ZnO was of high purity with low contamination from the starting precursors. Contamination usually causes aggregation of the nanoparticles into bigger clusters.

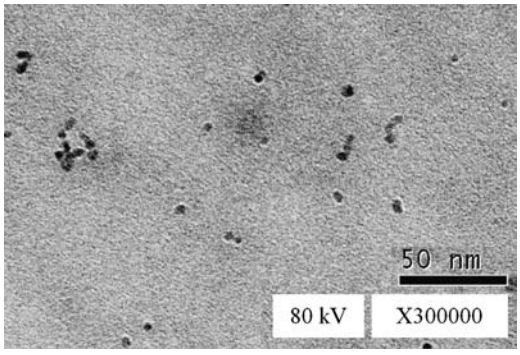

Fig. 4. TEM image of the ZnO synthesised in this study to be used as sensing receptor for the sensing probe.

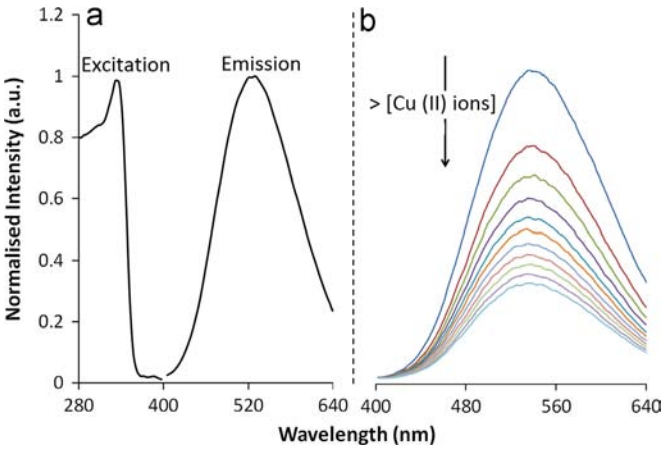

Fig. 5. The fluorescence spectra for the (a) optimum excitation and emission profile of the ZnO and (b) quenching effect towards the ZnO emission in the presence of increasing amount of Cu (II) ions.

The ZnO gave a strong emission at 535 nm when excited using the UV radiation (Fig. 5a). This matches with trend of the fluorescence emission of ZnO reported elsewhere [26–28]. This emission of the ZnO was significantly quenched in the presence of Cu (II) ions at the same excitation energy. Furthermore, the quenching showed a dependent trend towards the concentration of Cu (II) ions and thus can be utilised analytically for sensing purposes (Fig. 5b).

In addition, the studies observed no significant shift in the wavelength of the emission peak when altering the excitation energy. It was only noticeable with obvious intensity changes. Following this, the emission intensity at 535 nm was monitored with excitation ranging from 280–400 nm and was found that the cut off wavelength for the excitation was at 360 nm. Lower radiation energy towards the visible range had failed to excite the ZnO. The profile was overlaid with the output of the black light source used for the probe to ensure sufficient energy was provided to excite the ZnO (Fig. 6). The results show that the peak of power radiant emitted from the black light tube did not match exactly with the excitation peak of the ZnO. However both spectra overlapped very significantly at the band shoulder, which could still give an estimated excitation efficiency over 80%. This was further confirmed by the direct observation of bright light emitted from the ZnO sample when placed under the black light under dark environment (inset Fig. 6).

3.2. Probe optimisations and design

In order to reduce the cost and to make the probe more portable, rechargeable batteries were used as the power source. A low voltage indicator circuit was designed and integrated into the probe to indicate the level of the batteries power, a recharge will be required when the power is running low. This study found that the batteries gave a final voltage of 10.26 V with load on, when were fully discharged using a 500W inverter which consumed 0.51 A current. Once this was identified, the lowest voltage indicator for the probe was set to trigger at a slightly higher voltage of 10.40 V. This will allow a buffering period before the power ran total flat, and users would have sufficient time to make appropriate data back-up or to source for new batteries if more subsequent measurements were required. A red LED was used to signal the users when voltage runs below 10.40 V.

When the black light tube was switched on, the intensity was observed to increase steadily for the first 18 min and showed a stable intensity after that for up to at least an hour. The intensity of the lamp was recorded using the S3 sensor. Sufficient time was

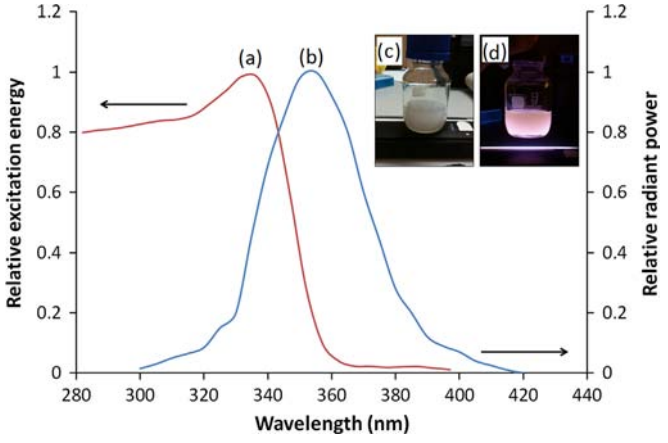

Fig. 6. The plot showing the (a) excitation energy efficiency of the ZnO at 535 nm over the range of 280–400 nm and (b) radiant power emitted from the black light used as excitation source in this study. Inset are the photographs of the ZnO under (c) normal room light and (d) under the black UV light.

required for the lamp to warm-up before reaching a stable signal. In fact, this applies to many of the conventional spectrophotometers where warming up of lamp is required before measurements can be made. Once the excitation light intensity had stabilised, the response time required for the Cu (II) ions detection was evaluated. This was performed by recording the time taken for the S1 and S2 sensors to reach plateau signals once the ZnO was added with a fixed amount of Cu (II) ions. By monitoring of the signal change over the duration of 5 min, it was found that the average time taken for S1 and S2 to reach plateau signal was around 35 s. Thus, this was set to be the response time and subsequent measurements were taken after this duration to promote better accuracy and precision of results.

Two photo-detectors (S1 and S2) were used to record the emission signal of the sample. This configuration promoted better accuracy since the average value was taken instead of from a single detector. Signals recorded from both the detectors were first normalised against the signals from the blank sample. Table 1 shows the normalised signals recorded by both the sensors from 5 samples with different concentrations of ZnO. From the data, the average variation in signal value was evaluated to be 0.64%. This certainly demonstrated the high reliability and accuracy of the setup of the probe. To counter check and to ensure both the sensors work accordingly during the later application stage, an algorithm was set to monitor the signal variation. Any variation of value from the two sensors that is larger than 0.80% will trigger a warning signal, while exceeding 1.00% variation will trigger an action signal. Thus, any fault of either one of the sensors or the non-homogenous distribution of sample in the chamber can be detected easily, avoiding it from propagating into giving inaccurate results.

Table 1
Comparison of signal recorded for detectors S1 and S2.

Sample	Normalised sensor reading		Average	Deviation	%Deviation
	Sensor 1 (S1)	Sensor 2 (S2)			
1	1.2379	1.2282	1.2282	0.0097	0.79
2	1.4765	1.4810	1.4788	0.0045	0.30
3	1.6687	1.6816	1.6752	0.0129	0.77
4	1.8721	1.8868	1.8795	0.0147	0.78
5	2.0666	2.0776	2.0721	0.0110	0.53
			Average deviation (%)		0.64

The probe was housed into a casing with a dimension of $10 \times 18 \times 16\ cm^3$ and a total weight less than 2 kg (Fig. 7). The display panel, main switch, warning indicators, and low power indicators were designed on top of the probe, while the sensing compartment was fixed on the side panel. The compact design promotes better portability for on-site measurements. The best distance alignment of the light source and the sensors away from the sensing windows were found to be 0.5 and 0.3 cm respectively (inset Fig. 7).

3.3. Optimisation of ZnO amount

The signals recorded by the probe showed an increment that was dependent towards the amount of ZnO added into the sample compartment. Since the emission will be effectively quenched in the presence of Cu (II) ions, it is necessary to ensure sufficient amount of ZnO before the addition of analyte. Thus this will give the highest intensity within the scale of the detectors for quenching to occur. This is to secure larger analytical window for later detection purpose. To achieve this, the ZnO was diluted with deionised water at different ratios and the corresponding signals were recorded. It was found that the signal had increased in the presence of more ZnO, but almost reaching plateau after the ratio of 1:20 ($ZnO:H_2O$, vol:vol). Self-quenching of the ZnO was suggested to be the main reason in the 'slowing-down' trend of the intensity increment as more ZnO was added. This was also observed in some other similar studies, which some even showed a decrease in the intensity at high concentration level of fluorophores [29]. Thus, for later sensing stage, a portion of ZnO from the stock solution was diluted with 20 portions of deionised water before it is used to detect Cu (II) ions.

3.4. Analytical characteristics

The emission intensity of the ZnO recorded from S1 and S2 was found to be quenched in the presence of Cu (II) ions in a concentration-dependent manner (Fig. 8). In order to predict the quenching mechanism, the addition of the Cu (II) ions was made at a slightly higher temperature of 30 °C instead of 25 °C. It was observed that the quenching was more profound suggesting a dynamic quenching between the ZnO and the Cu (II) ions. Higher temperature promotes greater kinetics and would definitely cause better interaction leading to greater quenching efficiency. Static quenching is unlikely in this case since higher temperature will promote dissociation of complex, which releases ZnO to its initial

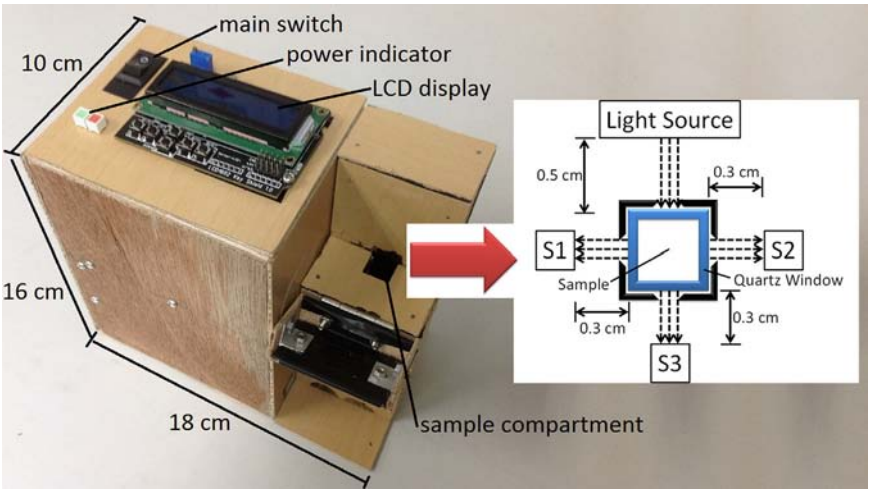

Fig. 7. The photograph of the miniature fluorescent probe with the diagram of a cross-section of the sensing compartment showing the position of the light source and detectors for S1, S2 and S3.

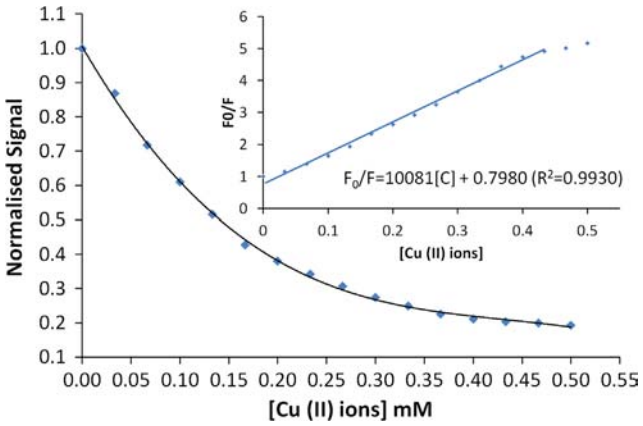

Fig. 8. The quenching trend of the intensity of ZnO in the presence of different concentrations of Cu (II) ions recorded from the probe. Inset is the linear correlation plot of the signal with the concentration of Cu (II) ions generated using the Stern–Volmer relationship.

stage without complexing with Cu (II) ions. Thus, it should promote emission instead of quenching. Based on these significant and consistent quenching patterns, the analytical potential of ZnO for the detection of Cu (II) ions using the miniature integrated probe was evaluated at room temperature. The quenching trend showed no linear correlation between the normalised signal and the concentration of the Cu (II) ions. Thus, modelling of the quenching trend was performed to establish a relationship that can be programmed into the microcontroller and later used to generate direct reading at the LCD readout panel. In this case, the standard Stern–Volmer relationship (Eq. (1)) that best describes the quenching profile of a fluorophore was adopted.

The normalised data after being modelled using the Eq. (1) was transformed into a linear correlation with the equation of $F_0/F = 10081[C] + 0.7980$ ($R^2 = 0.9930$) (inset Fig. 8). The relationship is linear up to the concentration of 0.45 mM of Cu (II) ions. The limit of detection (LOD) of the probe for the detection of concentration of Cu (II) ions was evaluated to be 7.68×10^{-7} M using Eq. (2).

$$\mathrm{LOD} = 3\sigma/s \tag{2}$$

where σ is the standard deviation of signal recorded from the blank ZnO sample ($n = 10$) and s is the slope of the calibration plot. This LOD value is compatible for many different applications such as water monitoring for the environment or for quality control in the copper related industries. Besides, the LOD achieved using this probe was lower and more sensitive when compared to some similar systems that utilised Q-Dots for sensing [16,30]. In addition, the probe performance was highly repeatable with an average standard deviation below 2.0% under the controlled study condition. The intensity of the ZnO was also observed to be stable under continuous exposure of the black UV light source. All these gave merits to the probe, which promoted robustness, more portable, cost effective, and sensitive towards the detection of Cu (II) ions. Since the ZnO used in this study was bare without surface modification, interference from the foreign chemical species within the matrix is possible. To overcome this, recalibration of the analytical response can be done quickly and easily to eliminate the potential of interference effect for real applications. The 'Standard Addition' protocol can be employed to perform the calibration, where stock solution of the Cu (II) ions will be added at an increasing amount to the sample matrix in the presence of the other foreign species as it is. Then the quenching effect will be recorded to establish the calibration curve. The newly obtained relationship for the dynamic response under this condition can be programmed into the microcontroller, which now can generate accurate concentration reading for the Cu (II) ions without effected by other interferences.

4. Conclusion

An integrated miniature fluorescent probe has been developed to leverage the sensing potential of ZnO for the detection of copper (II) ions. The probe has been constructed using low power circuit and sourced using rechargeable batteries. The probe is far cheaper than those conventional spectrofluorometers and even the mini-spectrophotometer. Even so, it does not compromise in its sensitivity as it can achieve the LOD down to sub micromolar range with the upper detection up to 0.45 mM. The work demonstrated the practicality of using Q-Dots as sensing receptor on-site, while not only limited to the elegant demonstration using expensive lab-based instrumentation. The probe has fast response time of 35 s, which allows rapid detection of Cu (II) ions.

Acknowledgements

This project was supported by the Faculty of Engineering, Computing and Science, Swinburne University of Technology Sarawak Campus. Partial financial supports were also obtained from Seed Grant 2-5243 and 2-5244 by the Swinburne University of Technology Sarawak Campus. The authors would like to acknowledge the support by all the staff, technicians, postgraduates and collaborators that have contributed to this study.

References

[1] I. Murkovic, A. Lobnik, G.J. Mohr, O.S. Wolfbeis, Anal. Chim. Acta 334 (1996) 125–132.
[2] Y. Xu, Y. Liu, X. Qian, J. Photochem. Photobiol. A 190 (2007) 1–8.
[3] H. Kuang, Y. Zhao, W. Ma, L. Xu, L. Wang, C. Xu, TRAC-Trends Anal. Chem. 30 (2011) 1620–1636.
[4] H.M.E. Azzazy, M.M.H. Mansour, S.C. Kazmierczak, Clin. Biochem. 40 (2007) 917–927.
[5] C. Shi, Y. Zhu, W.H. Cerwinka, H.E. Zhau, F.F. Marshall, J.W. Simons, S. Nie, L.W. K. Chung, Urol Oncol-Semin Ori. 26 (2008) 86–92.
[6] Y. Higuchi, M. Oka, S. Kawakami, M. Hashida, J. Controlled Release 125 (2008) 131–136.
[7] R.J. Byers, E.R. Hitchman, Prog. Histochem. Cytochem. 45 (2011) 201–237.
[8] A.M. Smith, H. Duan, A.M. Mohs, S. Nie, Adv. Drug Delivery Rev. 60 (2008) 1226–1240.
[9] A.F.E. Hezinger, J. Teßmar, A. Göpferich, Eur. J. Pharm. Biopharm. 68 (2008) 138–152.
[10] Z. Dai, J. Zhang, Q. Dong, N. Guo, S. Xu, B. Sun, Y. Bu, Chin. J. Chem. Eng. 15 (2007) 791–794.
[11] Y. Wang, L. Chen, Nanomed.-Nanotechnol. 7 (2011) 385–402.
[12] M. Ozkan, Drug Discovery Today 9 (2004) 1065–1071.
[13] W.R. Algar, A.J. Tavares, U.J. Krull, Anal. Chim. Acta 673 (2010) 1–25.
[14] M.P. Bruchez, Curr. Opinion Chem. Biol. 9 (2005) 533–537.
[15] R. Gui, X. An, H. Su, W. Shen, Z. Chen, X. Wang, Talanta 94 (2012) 257–262.
[16] M. Koneswaran, R. Narayanaswamy, Sens. Actuat. B-Chem. 139 (2009) 104–109.
[17] L.-Y. Zhang, H.-Z. Zheng, Y.-J. Long, C.-Z. Huang, J.-Y. Hao, D.-B. Zhou, Talanta 83 (2011) 1716–1720.
[18] J. Zhang, Y. Wan, Y. Li, Q. Zhang, S. Xu, H. Zhu, B. Shu, Environ. Pollut. 159 (2011) 1348–1353.
[19] D.-S. Xiang, G.-P. Zeng, Z.-K. He, Biosens. Bioelectron. 26 (2011) 4405–4410.
[20] C. Frigerio, D.S.M. Ribeiro, S.S.M. Rodrigues, V.L.R.G. Abreu, J.A.C. Barbosa, J.A. V. Prior, K.L. Marques, J.L.M. Santos, Anal. Chim. Acta 735 (2012) 9–22.
[21] M.E. Letelier, A.M. Lepe, M. Faúndez, J. Salazar, R. Marín, P. Aracena, H. Speisky, Chem.-Biol. Interact. 151 (2005) 71–82.
[22] V. Ochoa-Herrera, G. León, Q. Banihani, J.A. Field, R. Sierra-Alvarez, Sci. Total Environ. 412–413 (2011) 380–385.
[23] E.A. Meulenkamp, J. Phys. Chem. B 102 (1998) 5566–5572.
[24] Z. Hu, G. Oskam, P.C. Searson, J. Colloid Interface Sci. 263 (2003) 454–460.
[25] Y.L. Wu, A.I.Y. Tok, F.Y.C. Boey, X.T. Zeng, X.H. Zhang, Appl. Surf. Sci. 253 (2007) 5473–5479.
[26] D. Bera, L. Qian, S. Sabui, S. Santra, P.H. Holloway, Opt. Mater. 30 (2008) 1233–1239.
[27] L. Zhang, L. Yin, C. Wang, N. lun, Y. Qi, D. Xiang, J. Phys. Chem. C 114 (2010) 9651–9658.
[28] M.L. Singla, M. Shafeeq, M. Kumar, J. Lumin. 129 (2009) 434–438.
[29] S. Mohd Yazid, S. Chin, S. Pang, S. Ng, Microchim. Acta 180 (2013) 137–143.
[30] M. Algarra, B.B. Campos, B. Alonso, M.S. Miranda, Á.M. Martínez, C.M. Casado, J.C.G. Esteves da Silva, Talanta 88 (2012) 403–407.